ACS APPLIED MATERIALS & INTERFACES

RESEARCH ARTICLE

www.acsami.org

Reduction of Charge Recombination by an Amorphous Titanium Oxide Interlayer in Layered Graphene/Quantum Dots Photochemical Cells

HongBin Yang,[†] ChunXian Guo,[†] Guan Hong Guai,[†] QuanLiang Song,[‡] San Ping Jiang,[§] and Chang Ming Li*[,†,‡]

[†]School of Chemical and Biomedical and Center for Advanced Bionanosystems, Nanyang Technological University, 70 Nanyang Drive, Singapore 637457, Singapore

[‡]Institute for Clean Energy and Advanced Materials, Southwest University, Chongqing 400715, P. R. China

[§]Curtin Centre for Advanced Energy Science and Engineering, Department of Chemical Engineering, Curtin University of Technology, Perth, WA 6845, Australia

Supporting Information

ABSTRACT: The effect of an amorphous TiO_x interlayer on layered graphene/quantum dots photochemical cells has been investigated. The addition of the TiO_x interlayer eliminates the decay of photocurrent in the initial seconds after light illumination and significantly increases the slope of the steady-state photocurrent versus the light intensity. The open-circuit voltage decay measurements further illustrate a longer electron lifetime when an amorphous TiO_x interlayer is applied. Consequently, the photocurrent and photovoltage of the photovoltaic cell with a TiO_x interlayer are greatly increased. This work demonstrates that the graphene/amorphous TiO_x composite structure effectively inhibits charge recombination while enhancing charge transfer, providing a promising scaffold for quantum dots and dye-sensitized photovoltaic cells.

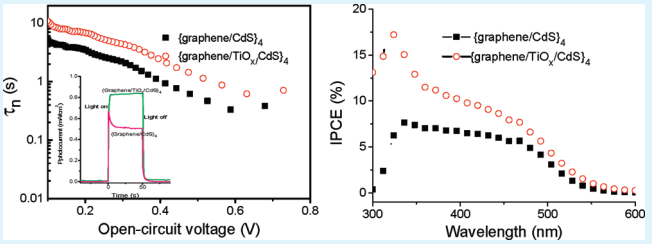

KEYWORDS: graphene, recombination, photochemistry, quantum dots, photovoltaic cells

INTRODUCTION

Graphene has attracted growing attention because of its unique properties such as a large specific surface area, high electric conductivity, and high transparency[1,2] and has been widely used in photovoltaic devices[3,4] and sensors,[5,6] as a supercapacitor,[7,8] as a catalyst,[9] for hydrogen storage,[10,11] and for flexible electronic circuits.[12]

Recently, a layered graphene/QDs photoanode has been used in quantum dots (QDs)-sensitized photovoltaic cells (QDSC),[13] demonstrating significant enhancement in the phototo-electron conversion efficiency contributed by its unique architecture, superior physicochemical properties, and favorable graphene work function. However, because the operation principle of graphene/QDs photovoltaic cells is similar to that of dye-sensitized solar cells (DSC),[14] it also suffers from losses of photogenerated electrons due to the recombination process.[15] Two interfacial recombination pathways are essential for the performance of the layered graphene/QDs photovoltaic cells. Electrons transported in the graphene layer injected from excited QD may recombine either (1) with the holes at the valence band of QDs or (2) with the redox couples in the electrolyte through direct contact.[14,16] To inhibit such recombination in the layered graphene/QD photochemical cell, we could use a barrier layer to separate the graphene layer (the electron transport layer) from the QDs and electrolyte. In DSC, different metal oxides such as ZnS, Al, ZrO, MgO_2, and amorphous TiO_2[17−20] film have been used to retard charge recombination for high-performance devices. However, such an interlayer for reducing the recombination process in a graphene/QDs device has never been investigated.

In this work, an amorphous TiO_x layer is introduced between graphene and QDs as a barrier layer by the dip coating method, and its effect on suppressing charge recombination is further investigated by the open-circuit voltage decay (OCVD) technique and incident light intensity-dependent photocurrent response profiles.

EXPERIMENTAL SECTION

Preparation of Materials and Fabrication of the Layered Photoanode. Graphene was synthesized by a modified Hummers method,[21,22] followed by hydrazine reduction as described previously.[13] The preparation of $\{graphene/TiO_x/CdS\}_n$ photoanodes is schematically depicted in Scheme 1, in which the precleaned ITO glass is coated with a thin layer of graphene by electrophoretic deposition at a constant current density of 0.5 mA/cm^2 in a 0.1 mg/mL graphene aqueous

Received: February 4, 2011
Accepted: April 29, 2011
Published: April 29, 2011

Scheme 1. Flow of $\{Graphene/TiO_x/CdS\}_n$ Photoanode Fabrication[a]

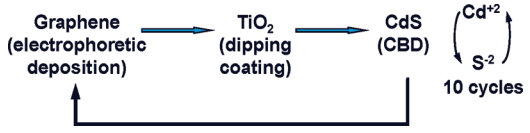

[a] *n* represents the number of repeating cycles (the cycle includes repeating steps 1−3).

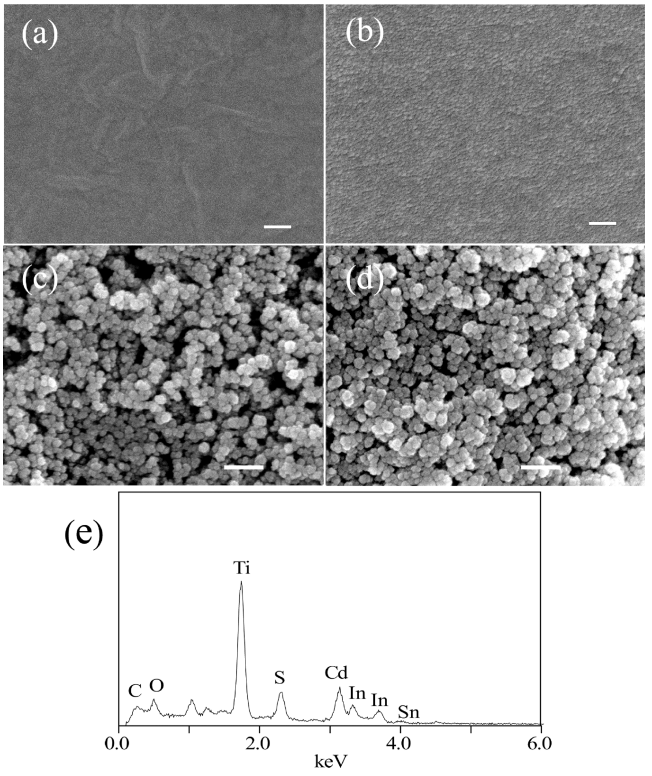

Figure 1. SEM images of (a) graphene on ITO, (b) TiO_x on a graphene surface, (c) CdS QDs grown on a graphene surface, and (d) CdS QDs grown on a graphene/TiO_x surface. (e) EDS of the $\{graphene/TiO_x/CdS\}_4$ photoanode. All scale bars are 100 nm.

solution for 50 s (film thickness of ~20 nm). Subsequently, the graphene-coated ITO glass is dipped into a titanium isopropoxide/2-propanol solution {TTIP, $Ti[OCH(CH_3)_2]_4$, Aldrich, 97.0%} to form an amorphous TiO_x layer.[23] To stabilize the TiO_x layer, the structure is heated at 60 °C for 10 min in air. Then, a layer of CdS QDs is directly synthesized on the prepared structure by sequential chemical bath deposition from their aqueous salt solutions of CdCl and NaS. Layered $\{graphene/TiO_x/QDs\}_n$ composite photoanodes are then fabricated by repeating steps 1−3 as one cycle. The number of cycles is represented by *n*.

Characterization of Materials. The morphology and structure of the layered photoanodes were investigated by FE-SEM (JSM-6700F), X-ray diffraction (D8 advance X-ray diffractometer, Bruker AXS, λ = 0.15418 nm). UV−vis absorption spectra were recorded using a spectrophotometer (UV-2450, Shimadzu). The compositions of the photoanodes were determined by energy dispersive X-ray spectroscopy (EDS, JSM-6700F).

Measurements of the Performance of the Photochemical Cell. The photochemical cell was constructed as shown in Figure S1 of the Supporting Information. A two-electrode system was used with a

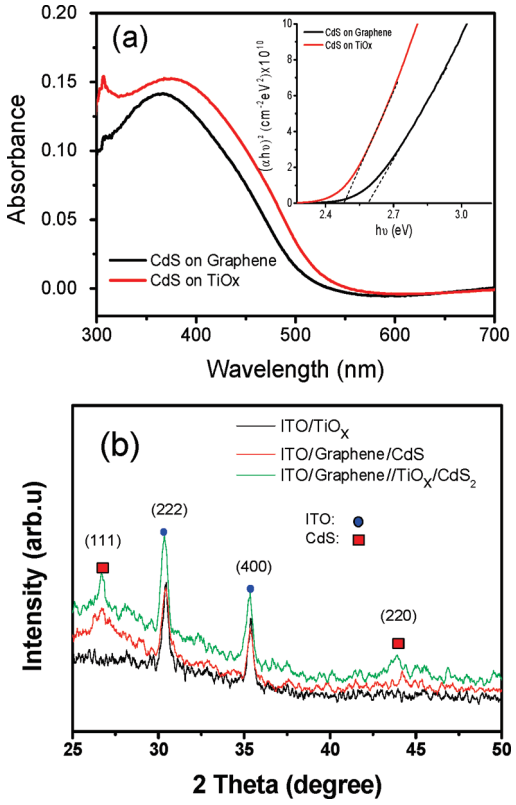

Figure 2. (a) UV−vis spectra of the CdS QDs film on ITO/graphene and ITO/graphene/TiO_x structures. The coating cycle of CdS QDs is 10. (b) X-ray diffraction spectra of the CdS QDs film on graphene and TiO_x nanoparticle-coated graphene surfaces.

photoanode having an area of 0.4 cm^2 and a platinum gauze of 1.0 cm^2 as the counter electrode. The electrolyte was a 0.1 M Na_2S aqueous solution. The photoresponses of devices were recorded using an Autolab potentiostat/galvanostat (PGSTAT30, Eco Chemie B.V., Utrecht, The Netherlands). The experiments were conducted using a 150 W Xe lamp (filtered, λ > 300 nm) as the light source. The illumination intensity near the electrode surface is 100 mW/cm^2. Neutral attenuation films were used to provide different incident power densities. Incident photon-to-electron conversion efficiency (IPCE) measurements were performed without bias illumination with respect to a calibrated silicon diode. The monochromic light was supplied by xenon light passing through a Cornerstone monochromator. A chopper was placed after the monochromator, and the signal was collected by Merlin lock-in radiometry after amplification by the current preamplifier.

RESULTS AND DISCUSSION

The surface morphologies of a graphene film on ITO, TiO_x-coated graphene, and CdS QDs on TiO_x-coated graphene were investigated using FE-SEM, showing Origami-like creases on ITO for the graphene sheets (Figure 1a) and a uniformly distributed TiO_x nanoparticle layer covered on the graphene surface (Figure 1b). However, after deposition of CdS QDs on both plain graphene and TiO_x/graphene surfaces, the QDs grown on the latter surface are slightly more dense than that on the former surface (Figure 1c,d), suggesting that the loading of CdS QDs is increased by the TiO_x coating possibly because of the higher absorbability of the Cd^{2+} on TiO_x surface. The composition of $\{graphene/TiO_x/CdS\}_4$ on ITO-coated glasses was further confirmed by EDS (Figure 1e).

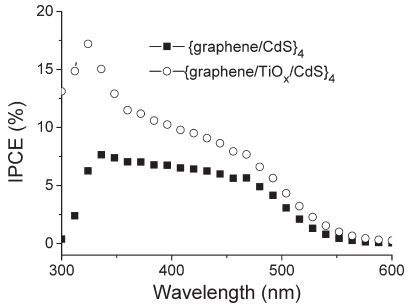

Figure 3. Photocurrent action spectra of photochemical cells with $\{graphene/TiO_x/CdS\}_4$ and $\{graphene/CdS\}_4$ photoanodes.

Figure 2a shows the absorption of CdS QDs grown on graphene and the TiO_x layer-coated graphene surface, of which the coating cycles of CdS QDs is 10. Compared with the absorption intensity of CdS QDs grown on a graphene surface, the absorption intensity of CdS QDs increases by 20% on TiO_x-coated graphene surface in the absorption region, and the absorption peak of CdS is shifted from 365 to 375 nm. The inset of Figure 2a shows the absorption edges of CdS QDs on graphene and amorphous TiO_x-coated graphene surfaces are 2.57 and 2.47 eV, respectively. The red shift of the absorption edge is ascribed to the quantum size effect,[24] implying that the crystal size of CdS QDs on the TiO_x layer is larger than that on the graphene surface. Figure 2b shows the X-ray diffraction (XRD) patterns of the TiO_x film and the CdS QDs films grown on graphene and TiO_x-coated graphene surfaces. Because no XRD peak can be observed form the TiO_x films, it indicates the films are amorphous. The peaks at 26.5° and 44° originate from the cubic phase of the CdS nanocrystal.[25] The higher peak intensity of the CdS QDs film on the TiO_x surface indicates that the crystallinity of CdS QDs is also improved by the TiO_x interlayer.

The influence of the insertion of TiO_x between graphene and QDs on the photoresponse of a single layered graphene/QDs photoanode was first investigated by various TTIP concentrations from 0.1 to 2.0 wt % in a 2-propanol solution. The results (Figure S2 of the Supporting Information) show that the $\{graphene/TiO_x/QDs\}_1$ photoanode with the TiO_x layer formed by a 0.5 wt % TTIP solution gives the best performance, in which the photocurrent and photovoltage of photochemical cells are enhanced by ~50 and ~15%, respectively, when compared to those of the graphene/QDs photoanode. Thus, 0.5 wt % TTIP was chosen for the subsequent experiments. Although the single TiO_x layer can enhance the photocurrent, it is low, especially at the low intensity of light, and cannot be used to accurately study the enhancement mechanism as shown in Figure S2 of the Supporting Information. Thus, the multilayer TiO_x structure was further used to investigate its buffer effect.

IPCE spectra of photochemical cells with $\{graphene/TiO_x/CdS\}_4$ and $\{graphene/CdS\}_4$ photoanodes are shown in Figure 3. With the presence of the TiO_x interlayer, IPCE of the photochemical cell is increased across the entire response range. The small peak at ~325 nm is most likely to be contributed from the inserting TiO_x layer and is supported by the presence of a photocurrent response from the photochemical cell with the $\{graphene/TiO_x\}_4$ photoanode shown in Figure S3 of the Supporting Information. Because a photocurrent of only 2 $\mu A/cm^2$ (at an illumination intensity of 100 mW/cm^2) is generated by the TiO_x interlayer, the enhancement of the IPCE of the photochemical cell

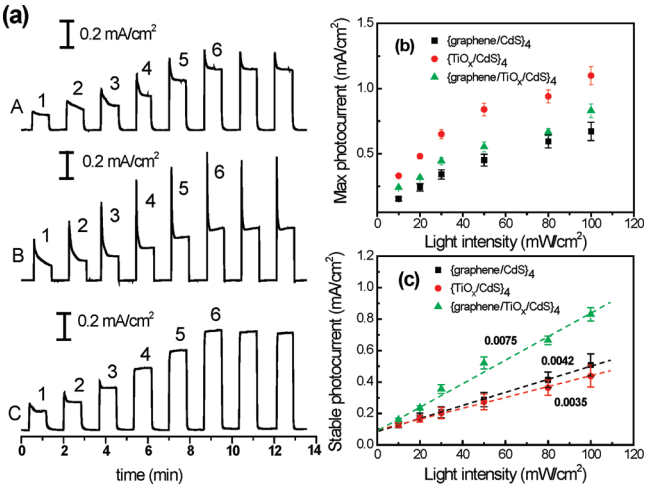

Figure 4. (a) Effect of excitation intensity on the stability of photocurrent generation of $\{graphene/CdS\}_4$ (A), $\{TiO_x/CdS\}_4$ (B), and $\{graphene/TiO_x/CdS\}_4$ (C) and photoanodes. Maximal photocurrent (b) and stable photocurrent (c) as a function of the intensity of incident light. The excitation intensity was maintained at (1) $0.1I_0$, (2) $0.2I_0$, (3) $0.3I_0$, (4) $0.5I_0$, (5) $0.8I_0$, or (6) I_0. The counter electrode was a platinum sheet. The electrolyte was 0.1 M Na_2S.

with a graphene/TiO_x/$CdS\}_4$ photoanode should be mainly attributed to an increased absorption of QDs or improved photogenerated electron collection[26] of the photoanode.

To understand the enhancement mechanism for the layered graphene/QDs photochemical cells by TiO_x interlayer coating, the relationship of the photocurrent responses for various photoanodes (A, {grpaphene/$CdS\}_4$; B, $\{TiO_x/CdS\}_4$; C, {graphene/TiO_x/$CdS\}_4$) with different incident light densities was investigated. As illustrated in Figure 4a, the photocurrent response profiles for the three kinds of photoanodes under irradiation are quite different, in which the photocurrent responses of both photochemical cells A and B show fast decay until reaching light intensity I_0, at which the photocurrents decay by approximately 25 and 60% and then become stable over the entire applied light intensity range. However, the photocurrent response of photochemical cell C shows only the decay process at low illumination intensities ($<0.3I_0$). At higher illumination intensities, the decay process disappears. The photocurrent is actually the number of charges collected by the photoanode, and its decay with irradiation time signifies a proportional loss of photogenerated charges from either charge trapping in the acceptor layer[27,28] (trapped in the graphene or TiO_x layer) or an enhanced recombination process like that reported previously.[14,29] In addition, the correlations between the maximal photocurrents of the three photochemical cells and different illumination intensities in Figure 4b (photovoltage as a function of illumination intensity shown in Figure S4 of the Supporting Information) show the same increasing trend with an increase in the illumination intensity. The maximal photocurrent difference among the three photoanodes indicates the electrodes possess different CdS QDs loadings and CdS QD/electrolyte contact areas. The maximal transient photocurrent can represent the number of excitons generated by the photoanode. From Figure 4, the $\{graphene/CdS\}_4$ photoanode increases the maximal transient current by ~23% via addition of the TiO_x interlayer, which is almost the same enhanced 20% absorption intensity shown in Figure 2. Furthermore, a linear relationship of the stable photocurrent for the three photochemical cells versus the illumination

Scheme 2. Schematic Representation of Photogenerated Electron Transfer Processes in a Layered Graphene (Gr)/QDs Structure with a TiO_x Interlayer (a) and the Energy Band Diagram (b), Showing the Main Electronic Processes at the Interface in QDs[a]

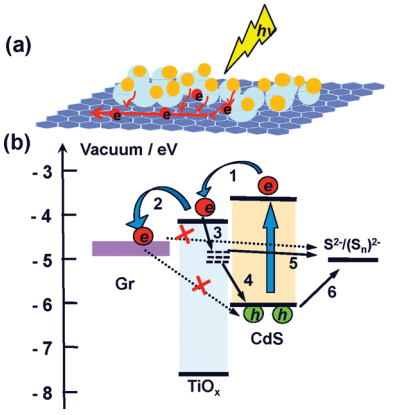

[a] (1) Electron injection, (2) electron transfer, (3) trapping of the electron at surfaces states, the two charge recombination pathways of trapped electron recombination with (4) the hole at the valence band of QDs and (5) the oxidized redox couple, and (6) hole extraction. The recombination between the electron at the Fermi level of graphene and the hole at the valence band of QDs and the oxidized redox couple was inhibited by the TiO_x layer. The electrolyte was 0.1 M Na_2S (with S^{2-}/Sn^{2-} redox couples). The energy levels of CdS, TiO_x, and graphene were taken from refs 23 and 43−45.

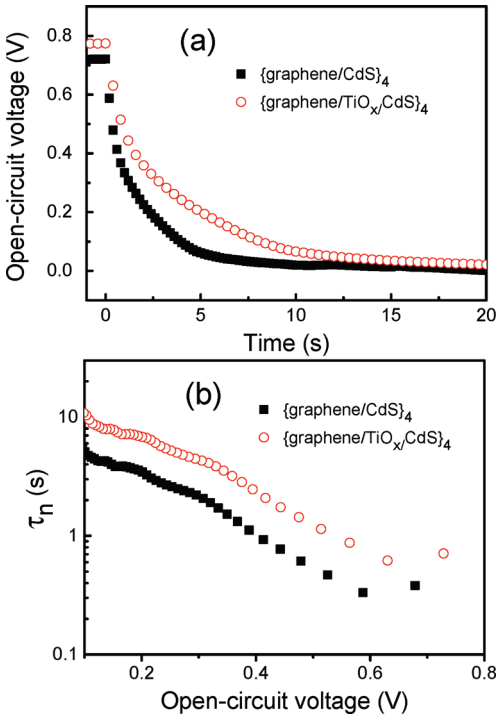

Figure 5. (a) Open-circuit voltage decay profiles and (b) electron lifetime as a function of the open-circuit voltage (V_{oc}) of the photochemical cell with and without a TiO_x layer.

intensity is observed over the entire light intensity range (Figure 4c) of which the fitted slope for photochemical cell C is 0.0075, which is larger than that of cell A (0.0042) or cell B (0.0035). Thus, I_{sc} is further increased by 60%, from 0.51 to 0.83 mA/cm^2, at an illumination intensity of 100 mW/cm^2. This enhancement is 3 times greater than that caused by the increased absorption intensity of the photoanode. The improved I_{sc} and elimination of the decay in photocurrent provide persuasive evidence that the presence of an amorphous TiO_x interlayer in the layered graphene/QDs photoanode reduces electron loss and significantly enhances the charge collection efficiency, which are in good agreement with the IPCE results. The transient photocurrent of a photoelectrode can be used to quantitatively analyze the electrode−electrolyte interface reaction kinetics.[30,31] However, it is not used in this work because the decay of the transient photocurrent of the photoanode with the TiO_x interlayer is totally eliminated.

Scheme 2 represents the photogenerated electron transfer process in the layered graphene/QDs structure with a TiO_x interlayer and the corresponding energy band diagram. Via introduction of the TiO_x layer, the recombination events between the electrons at the Fermi level of graphene with both the holes at the valence band of QDs and the redox couples are inhibited, which is supported by the enhanced performance of the {graphene/TiO_x/CdS}$_4$ photochemical cell. However, it has been reported[32,33] that the transfer of charge in the TiO_2 nanoparticle layer occurs via electron hopping between the trap states. Such a conducting pathway tends to trap the charges by the TiO_2 trap states (bandgap and surface states).[34−36] Consequently, recombination pathways (4 and 5 as shown in Scheme 2) would be introduced into the charge transfer process. The trap state-assisted recombination between the injected electron in the TiO_x layer and the hole at the valence band of QDs (or dye) and oxidized redox couples has been studied by using transient spectroscopic techniques.[28,34,37,38] The observed rapid decay of photocurrent in photochemical cell B with the {TiO_x/CdS}$_4$ photoanode (Figure 4a, trace B) further supports the proposed recombination mechanism in the TiO_x layer. Our measurements are consistent with Kamat's works,[39,40] which also show a fast decay followed by a stable photocurrent under illumination. The charge loss induced by the trap state-assisted recombination in photochemical cell B (60%) is larger than that in cell A (25%), but for photochemical cell C with the {graphene/TiO_x/CdS}$_4$ photoanode, the larger I_{sc} and elimination of the photocurrent decay indicate that trap state-assisted recombination does not occur during charge transfer. The results can be explained. Recent works[41,42] have demonstrated the transport of electrons from the semiconductor to graphene via a stepwise transfer process with a fast shuttling rate. Because of the high conductivity of graphene and its stepwise energy difference with respect to TiO_x, electrons injected from excited QDs would be transferred directly from the TiO_x conducting band to the adjacent graphene layer before they are trapped by the trap states in the amorphous TiO_x layer. Thus, the trap state-assisted recombination is retarded for a better charge collection in the device.

To further demonstrate that an amorphous TiO_x interlayer can retard the charge recombination in a layered {graphene/QDs} photochemical cell, the electron lifetime (τ_n) of the device was measured by the open-circuit voltage decay (OCVD) technique. The electron lifetime in a photochemical cell has been widely derived from the OCVD measurement[46,47] and has used as a kinetic parameter to obtain useful information about the electron recombination rate. The OCVD measurement was conducted by turning off the illumination on the photoanode in a steady state to monitor the subsequent decay of the open-circuit voltage (V_{oc}).

The τ_n can be obtained by the reciprocal of the derivative of the decay curve normalized by the thermal voltage using the following equation:

$$\tau_n = -\frac{k_B T}{e}\left(\frac{dV_{oc}}{dt}\right)^{-1}$$

where k_B is Boltzmann's constant, T is the absolute temperature, e is the positive elementary charge, and dV_{oc}/dt is the derivative of the transient open-circuit voltage. The decay of V_{oc} reflects the decrease in the electron concentration in the photoanode,[14] which is mainly caused by charge recombination. Figure 5a shows the OCVD decay curves of photochemical cells with and without a TiO_x layer, showing clearly that the OCVD response of the photochemical cell with the TiO_x interlayer is much slower than that without TiO_x. Accordingly, the photoanode has a longer electron lifetime over the entire range of open-circuit voltage (Figure 5b), suggesting that the electrons injected from excited CdS QDs can survive for a longer period without recombination for fast electron transfer in the $\{graphene/TiO_x/CdS\}_4$ photoanode. The OCVD measurements further support the possibility that photogenerated electron recombination is effectively retarded by the TiO_x interlayer.

CONCLUSIONS

In summary, an amorphous TiO_x layer has been successfully incorporated into a layered graphene/QDs structure for a photovoltaic cell. The amorphous TiO_x interlayer serves as a barrier to reduce the level of charge recombination by separating the graphene layer from the oxidized QDs and redox couples in the electrolyte. With the interlayer, the decay of photocurrent in the initial seconds of illumination is eliminated at high incident intensities. Thus, the photocurrent and photovoltage of a photochemical cell using the graphene/TiO_x/QDs layers are enhanced by 60 and 10%, respectively. This study clearly demonstrates that the TiO_x interlayer in the graphene/TiO_x composite structure for QDs photovoltaic cells and DSCs can enhance charge transfer while reducing the level of charge recombination. Moreover, the low-temperature, solution-based, and low-cost fabrication process of graphene/TiO_x composites is favorable for mass-produced flexible plastic photoanodes.

ASSOCIATED CONTENT

Supporting Information. Experimental details, scheme of the setup of the photochemical cell (Figure S1), dependence of the photocurrent and photovoltage of $\{graphene/TiO_x/CdS\}_1$ photoanodes on the concentration of TTIP (Figure S2), photocurrent and photovoltage of the $\{graphene/TiO_x\}_4$ photoanode (Figure S3), photocurrent transient profiles of different photoanodes (Figure S4), and dependence of the photovoltage on the intensity of incident light (Figure S5). This material is available free of charge via the Internet at http://pubs.acs.org.

AUTHOR INFORMATION

Corresponding Author
*E-mail: ecmli@ntu.edu.sg.

ACKNOWLEDGMENT

We are grateful for financial support from the Agency of Science, Technology and Research (A*Star), Singapore (SERC Grant 072 134 0054), and the Institute for Clean Energy and Advanced Materials, Southwest University.

REFERENCES

(1) Li, X.; Zhu, Y.; Cai, W.; Borysiak, M.; Han, B.; Chen, D.; Piner, R. D.; Colombo, L.; Ruoff, R. S. *Nano Lett.* **2009**, *9*, 4359.
(2) Geim, A. K.; Novoselov, K. S. *Nat. Mater.* **2007**, *6*, 183.
(3) Wang, X.; Zhi, L.; Mullen, K. *Nano Lett.* **2008**, *8*, 323.
(4) Hu, Y. H.; Wang, H.; Hu, B. *ChemSusChem* **2010**, *3*, 782.
(5) Schedin, F.; Geim, A. K.; Morozov, S. V.; Hill, E. W.; Blake, P.; Katsnelson, M. I.; Novoselov, K. S. *Nat. Mater.* **2007**, *6*, 652.
(6) Guo, C. X.; Lu, Z. S.; Lei, Y.; Li, C. M. *Electrochem. Commun.* **2010**, *12*, 1237.
(7) Biswas, S.; Drzal, L. T. *ACS Appl. Mater. Interfaces* **2010**, *2*, 2293.
(8) Wang, H.; Hao, Q.; Yang, X.; Lu, L.; Wang, X. *ACS Appl. Mater. Interfaces* **2010**, *2*, 821.
(9) Cao, L.; Liu, Y.; Zhang, B.; Lu, L. *ACS Appl. Mater. Interfaces* **2010**, *2*, 2339.
(10) Wang, Y.; Guo, C. X.; Wang, X.; Guan, C.; Yang, H.; Wang, K.; Li, C. M. *Energy Environ. Sci.* **2011**, *4*, 195.
(11) Lee, H.; Ihm, J.; Cohen, M. L.; Louie, S. G. *Nano Lett.* **2010**, *10*, 793.
(12) Liang, J.; Chen, Y.; Xu, Y.; Liu, Z.; Zhang, L.; Zhao, X.; Zhang, X.; Tian, J.; Huang, Y.; Ma, Y.; Li, F. *ACS Appl. Mater. Interfaces* **2010**, *2*, 3310.
(13) Guo, C. X.; Yang, H. B.; Lu, Z. S.; Song, Q. L.; Sheng, Z. M.; Li, C. M. *Angew. Chem., Int. Ed.* **2010**, *49*, 3014.
(14) Mora-Seró, I.; Giménez, S.; Fabregat-Santiago, F.; Gómez, R.; Shen, Q.; Toyoda, T.; Bisquert, J. *Acc. Chem. Res.* **2009**, *42*, 1848.
(15) Song, Q. L.; Yang, H. B.; Gan, Y.; Gong, C.; Ming Li, C. *J. Am. Chem. Soc.* **2010**, *132*, 4554.
(16) Hodes, G. *J. Phys. Chem. C* **2008**, *112*, 17778.
(17) Shen, Q.; Kobayashi, J.; Diguna, L. J.; Toyoda, T. *J. Appl. Phys.* **2008**, *103*, 084304.
(18) Fabregat-Santiago, F.; Garcia-Canadas, J.; Palomares, E.; Clifford, J. N.; Haque, S. A.; Durrant, J. R.; Garcia-Belmonte, G.; Bisquert, J. *J. Appl. Phys.* **2004**, *96*, 6903.
(19) Kitiyanan, A.; Ngamsinlapasathian, S.; Pavasupree, S.; Yoshikawa, S. *J. Solid State Chem.* **2005**, *178*, 1044.
(20) Grinis, L.; Kotlyar, S.; Rühle, S.; Grinblat, J.; Zaban, A. *Adv. Funct. Mater.* **2010**, *20*, 282.
(21) Hummers, W. S.; Offeman, R. E. *J. Am. Chem. Soc.* **1958**, *80*, 1339.
(22) Stankovich, S.; Dikin, D. A.; Piner, R. D.; Kohlhaas, K. A.; Kleinhammes, A.; Jia, Y.; Wu, Y.; Nguyen, S. T.; Ruoff, R. S. *Carbon* **2007**, *45*, 1558.
(23) Kim, J.; Kim, S.; Lee, H. H.; Lee, K.; Ma, W.; Gong, X.; Heeger, A. *Adv. Mater.* **2006**, *18*, 572.
(24) Gorer, S.; Hodes, G. *J. Phys. Chem.* **1994**, *98*, 5338.
(25) Nicolau, Y. F.; Dupuy, M.; Brunel, M. *J. Electrochem. Soc.* **1990**, *137*, 2915.
(26) Yang, H.; Song, Q.; Lu, Z.; Guo, C.; Gong, C.; Hu, W.; Li, C. M. *Energy Environ. Sci.* **2010**, *3*, 1580.
(27) Howe, R. F.; Gratzel, M. *J. Phys. Chem.* **1985**, *89*, 4495.
(28) Kang, S. H.; Kim, J.-Y.; Sung, Y.-E. *Electrochim. Acta* **2007**, *52*, 5242.
(29) Peter, L. *Acc. Chem. Res.* **2009**, *42*, 1839.
(30) Schlettwein, D.; Jaeger, N. I. *J. Phys. Chem.* **1993**, *97*, 3333.
(31) Abe, T.; Kamei, Y.; Nagai, K. *Solid State Sci.* **2010**, *12*, 1136.
(32) Bisquert, J. *J. Phys. Chem. C* **2007**, *111*, 17163.
(33) Anta, J. A.; Nelson, J.; Quirke, N. *Phys. Rev. B* **2002**, *65*, 125324.
(34) Salvador, P. *Surf. Sci.* **1987**, *192*, 36.

(35) de Jongh, P. E.; Vanmaekelbergh, D. *Phys. Rev. Lett.* **1996**, *77*, 3427.
(36) Mora-Seró, I.; Bisquert, J. *Nano Lett.* **2003**, *3*, 945.
(37) Kopidakis, N.; Neale, N. R.; Zhu, K.; van de Lagemaat, J.; Frank, A. J. *Appl. Phys. Lett.* **2005**, *87*, 202106.
(38) Hagfeldt, A.; Lindström, H.; Södergren, S.; Lindquist, S.-E. *J. Electroanal. Chem.* **1995**, *381*, 39.
(39) Robel, I.; Subramanian, V.; Kuno, M.; Kamat, P. V. *J. Am. Chem. Soc.* **2006**, *128*, 2385.
(40) Bang, J. H.; Kamat, P. V. *Adv. Funct. Mater.* **2010**, *20*, 1970.
(41) Ng, Y. H.; Lightcap, I. V.; Goodwin, K.; Matsumura, M.; Kamat, P. V. *J. Phys. Chem. Lett.* **2010**, *1*, 2222.
(42) Yang, N.; Zhai, J.; Wang, D.; Chen, Y.; Jiang, L. *ACS Nano* **2010**, *4*, 887.
(43) Gratzel, M. *Nature* **2001**, *414*, 338.
(44) Liu, Z.; Liu, Q.; Huang, Y.; Ma, Y.; Yin, S.; Zhang, X.; Sun, W.; Chen, Y. *Adv. Mater.* **2008**, *20*, 3924.
(45) Czerw, R.; Foley, B.; Tekleab, D.; Rubio, A.; Ajayan, P. M.; Carroll, D. L. *Phys. Rev. B* **2002**, *66*, 033408.
(46) Zaban, A.; Greenshtein, M.; Bisquert, J. *ChemPhysChem* **2003**, *4*, 859.
(47) Bisquert, J.; Zaban, A.; Greenshtein, M.; Mora-Seró, I. *J. Am. Chem. Soc.* **2004**, *126*, 13550.